CHEMISTRY
A EUROPEAN JOURNAL

DOI: 10.1002/chem.200600683

Unexpected Conformational Properties of 1-Trifluoromethyl-1-Silacyclohexane, $C_5H_{10}SiHCF_3$: Gas Electron Diffraction, Low-Temperature NMR Spectropic Studies, and Quantum Chemical Calculations**

Georgiy V. Girichev,[a] Nina I. Giricheva,[b] Andras Bodi,[c] Palmar I. Gudnason,[c] Sigridur Jonsdottir,[c] Agust Kvaran,[c] Ingvar Arnason,*[c] and Heinz Oberhammer*[d]

Abstract: The molecular structure of axial and equatorial conformers of 1-trifluoromethyl-1-silacyclohexane, ($C_5H_{10}SiHCF_3$), as well as the thermodynamic equilibrium between these species was investigated by means of gas electron diffraction (GED), dynamic nuclear magnetic resonance (DNMR) spectroscopy, and quantum chemical calculations (B3LYP, MP2, and CBS-QB3). According to GED, the compound exists as a mixture of two C_s symmetry conformers possessing the chair conformation of the six-membered ring and differing in the axial or equatorial position of the CF_3 group (axial = 58(12) mol%/equatorial = 42(12) mol%) at $T = 293$ K. This result is in a good agreement with the theoretical prediction. This is, however, in sharp contrast to the conformational properties of the cyclohexane analogue. The main structural feature for both conformers is the unusually long exocyclic bond length Si–C 1.934(10) Å. A low-temperature ^{19}F NMR experiment results in an axial/equatorial ratio of 17(2) mol%:83(2) mol% at 113 K and a $\Delta G^{\neq}$ of 5.5(2) kcal mol^{-1}. CBS-QB3 calculations in the gas-phase and solvation effect calculations using the PCM(B3LYP/6-311G*) and IPCM-(B3LYP/6-311G*) models were applied to estimate the axial/equatorial ratio in the 100–300 K temperature range, which showed excellent agreement with the experimental results. The minimum energy pathways for the chair-to-chair inversion of trifluoromethylsilacyclohexane and methylsilacyclohexane were also calculated using the STQN-(Path) method.

Keywords: conformation analysis · electron diffraction · NMR spectroscopy · quantum chemical calculations · silacyclohexane

Introduction

The conformational behavior of six-membered ring systems, steric effects of substituents, and stereoelectronic interactions in the ring systems continue to be an active field of research.[2–8] Cyclohexane and its derivatives play an important role in organic stereochemistry. The Gibbs free energy difference between axial and equatorial conformations in monosubstituted cyclohexanes has been used as a measure of the inherent conformational parameters of the substituent. With the rare exception of substituents, which are connected via mercury to the cyclohexane ring, a general preference for the equatorial conformer is found.[9] Consequently, a positive A value (see Scheme 1 for definition of A) corresponds to a preference for the equatorial conformer. The equatorial preference of Me, Et, and *i*Pr as substituents on cyclohexane has been reinvestigated recently. The A value of the methyl group was found to be 1.80(2) kcal mol^{-1} by low-temperature ^{13}C NMR spectroscopy and 1.98 kcal mol^{-1} by high-level ab initio calculations.[10]

[a] Prof. Dr. G. V. Girichev
Ivanovo State University of Chemistry and Technology
Ivanovo 153460 (Russia)

[b] Prof. Dr. N. I. Giricheva
Ivanovo State University, Ivanovo 153025 (Russia)

[c] A. Bodi, P. I. Gudnason, Dr. S. Jonsdottir, Prof. Dr. A. Kvaran, Prof. Dr. I. Arnason
Science Institute, University of Iceland, Dunhaga 3
107 Reykjavik (Iceland)
Fax: (+354) 552-8911
E-mail: ingvara@raunvis.hi.is

[d] Prof. Dr. H. Oberhammer
Institut für Physikalische und Theoretische Chemie
Universität Tübingen, Auf der Morgenstelle 8
72076 Tübingen (Germany)
Fax: (+49) 7071-295490
E-mail: heinz.oberhammer@uni-tuebingen.de

[**] Conformations of Silicon-Containing Rings, Part 6; for Part 5 see ref. [1].

Supporting information for this article is available on the WWW under http://www.chemeurj.org/ or from the author.

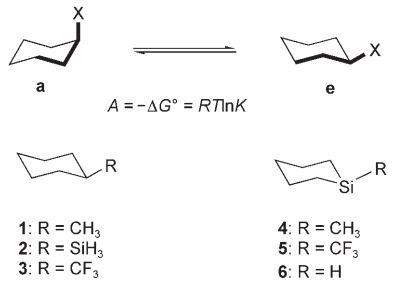

Scheme 1.

Silylcyclohexane **2** and 1-methyl-1-silacyclohexane **4** are the two simplest Si analogues of methylcyclohexane **1**. The *A* value of the silyl group was found by ^{1}H and ^{13}C NMR spectroscopy to be 1.45 and 1.44 kcal mol^{-1}, respectively, at 188 K.[11] From a gas electron diffraction (GED) experiment Shen et al. reported a conformational mixture of equatorial (90 ± 10 %) and axial forms at 75 °C.[12] Cho et al. have compared calculated *A* values for the methyl and silyl groups on cyclohexane.[13] They reported *A* values of 2.14 kcal mol^{-1} (CH_3) and 1.90 kcal mol^{-1} (SiH_3) from ab initio calculations, whereas MM3 calculations resulted in 1.78 (CH_3) and 1.16 kcal mol^{-1} (SiH_3). The authors explain the lower *A* value of the silyl group compared with the methyl group by the longer Si–C bond (1.904 Å) compared to the C–C bond (1.534 Å), which makes the axial SiH_3 sterically less unfavorable than the axial methyl group.

In the past, the *A* value of **4** have been reported to be negative from investigations using ^{1}H NMR measurements at room temperature,[14] as well as force field calculations.[15,16] In a recent investigation we were able to show from GED, low-temperature NMR, and quantum chemical (QC) calculations that **4** truly has a positive *A* value, albeit a much lower one than **1** and **2**. Our results were 0.45(14) (GED), 0.23(2) (^{13}C NMR at 110 K), and 0.46–0.60 kcal mol^{-1} (QC, depending on method and basis set).[1] In a subsequent paper we then described the gas-phase structure and conformational properties of 1-silabutane and 2-silabutane.[17] The *gauche* conformer in *n*-butane, 1-silabutane, and 2-silabutane is related to the axial conformer in **1**, **2**, and **4**, respectively (as indicated in Scheme 1), and likewise is the *anti* conformer of the butanes related to the equatorial ring conformer. It was remarkable to see that substituting CH_3 in **1** or *n*-butane for SiH_3 in **2** or 1-silabutane results in considerably longer (ca 0.3 Å) H–H distances in the axial and *gauche* conformers, respectively, whereas ΔH (axial–equatorial and *gauche–anti*, respectively) between the two conformers remains similar. Going from **2** to **4** or from 1-silabutane to 2-silabutane resulted in a moderately longer H–H distance (0.1–0.2 Å); at the same time ΔH decreases dramatically. There is no obvious explanation for this behavior; therefore we would like to add more knowledge to this field. The trifluoromethyl group is an interesting alternative to the methyl group and we started this investigation by carrying out preliminary calculations on the relative energies for axial and equatorial conformers of the silacyclohexane derivate **5**. Surprisingly, we found both conformers to be of similar energy, which was unexpected considering the high *A* value (2.5 kcal mol^{-1}) of the cyclohexane analogue **3**.[18] From this background we were prompted to synthesize the hitherto unknown compound **5** and explore its conformational behavior by experimental means. In the present paper we report a conformational analysis for **5** using GED, low-temperature ^{19}F NMR spectroscopy, and quantum chemical calculations.

Results and Discussion

GED Analysis: Structure refinements were carried out with least squares analyses of the experimental sM(*s*) function. According to quantum chemical calculations, two stable conformers of $C_5H_{10}SiHCF_3$ exist (Figure 1), that is, axial (**5a**) and equatorial (**5e**). Each form possesses C_s symmetry with chair conformation of the six-membered ring. Figure 2 shows the theoretical radial distribution functions f(*r*) for the two conformers **5a** and **5e**. The theoretical function of each conformer was derived with the calculated (B3LYP/6-31G**) geometrical parameters and vibrational amplitudes. Both functions differ appreciably in the range $r > 3$ Å, which contains the peaks corresponding to long nonbonded distances between the atoms of the CF_3 group and the atoms of the six-membered ring. This demonstrates that the electron diffraction intensities are sensitive to the conformational properties of this compound. Comparison with the experimental radial distribution function f(*r*) derived by Fourier transformation of the molecular intensities sM*(s)* demonstrates that both conformers are present in vapor under the conditions of the GED experiment.

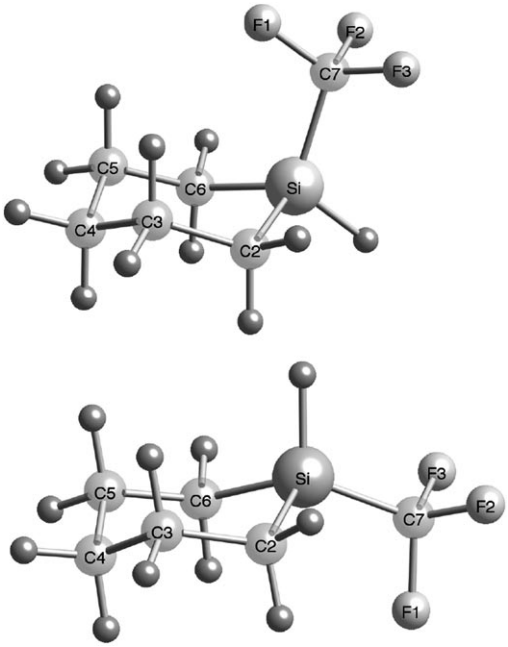

Figure 1. Structural models of axial **5a** (above) and equatorial **5e** (below) conformers for 1-trifluoromethyl-silacyclohexane with atom numbering.

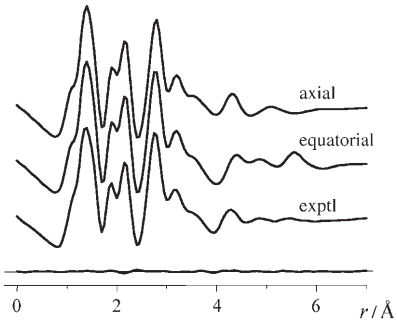

Figure 2. Radial distribution functions for calculated (B3LYP/6-31G**) geometries of axial conformer **5a** and equatorial conformer **5e**, experimental function and difference curve for mixture.

Conventional least squares analyses of sM(*s*) were carried out using the modified version of the KCED program.[19] Scattering amplitudes and phases of reference [20] were used. The following assumptions, which are based on the quantum chemical calculations (B3LYP/6-31G**) were made to describe the geometry of the two conformers (atom numbering is given in Figure 1): 1) Chair conformation of the ring with C_s overall symmetry. The difference between the C–C bonds [(C2–C3)–(C3–C4)] was constrained to the calculated value. 2) C–H bond lengths and H-C-H bond angles of all CH_2 groups were assumed to be equal, and the H-C-H angles were set to the calculated value. Calculated C–H bond lengths deviate by less than 0.003 Å from their mean value and H-C-H bond angles by less than 0.2°. The CH_2 groups at carbon atoms C3, C4 and C5 were assumed to be oriented symmetrical to the bisector of the adjacent endocyclic angle. Calculated deviations from this exact symmetrical orientation (rocking, wagging and twisting angles) are less than 1°. The rocking and twisting angles for the CH_2 groups at carbon atoms C2 and C6, which are larger than 1°, were set to calculated values. 3) The CF_3 group was constrained to C_s symmetry with equal F-C-F angles. The tilt angle was set to zero and the difference between the two C–F bond lengths [(C7–F1)–(C7–F2)] was fixed to the theoretical difference. 4) The Si–H bond length and C2-Si-H bond angle were constrained to calculated values. With the above assumptions, 11 geometric parameters were used to construct the geometry of the compound in the least squares analyses, five bond lengths (Si–C2, Si–C7, C2–C3, C7–F1, C–H), four bond angles (C2-Si-C6, Si-C2-C3, C2-Si-C7, Si-C7-F), the flap angle of the C4 atom out of the plane of the C2,C3,C5,C6 atoms and the torsional angle around the Si–C2 bond (ϕ(C6-Si-C2-C3)). The 11 structural parameters (p_1 to p_{11} in Table 1) of the axial conformer were refined simultaneously and independently together with 11 groups of vibrational amplitudes. The differences between vibrational amplitudes within each group were set to the calculated differences. In the least squares fitting of the molecular intensities the geometrical parameters of the equatorial form were tied to those of the axial conformer using the calculated differences and the theoretical vibrational amplitudes. Starting values for bond distances and angles were taken from the B3LYP/6-31G** calculations, those for vibrational amplitudes as well as the vibrational corrections, $\Delta r = r_{h1} - r_a$, for both conformers were derived from calculated (B3LYP/6-31G**) force fields using the approach of Sipachev incorporated in the program SHRINK.[21]

Table 1. Experimental and calculated geometric parameters of axial conformer **5a** of $C_5H_{10}SiHCF_3$ [Å and °]. Atom numbering is given in Figure 1. Error limits are $3\sigma_{LS}$ values.

	GED r_{h1} structure	B3LYP/6-31G** r_e structure	MP2/6-31G** r_e structure
Si–C2 p_1[a]	1.856(3)	1.885	1.876
ΔSiC p_2	0.078(10)	0.048	0.050
Si–C7 (p_1, p_2)	1.934(10)	1.931	1.923
C2–C3 p_3	1.546(2)	1.548	1.540
C3–C4 (p_3)	1.539(2)	1.540	1.532
C7–F1 p_4	1.360(2)	1.363	1.366
C7–F2 (p_4)	1.353(2)	1.360	1.362
$(C-H)_{mean}$ p_5	1.122(5)	1.098	1.093
Si–H	1.487[d]	1.488	1.479
C2-Si-C6 p_6	106.7(18)	106.3	105.9
Si-C2-C3 p_7	112.4(10)	110.4	109.6
C2-C3-C4	114.4(12)	114.0	113.6
C3-C4-C5	113.6(21)	114.6	114.2
C2-Si-C7 p_8	108.2(9)	110.5	110.1
Si-C7-F1 p_9	112.5(2)	112.0	111.5
tilt (CF3)[b]	0.0[d]	−0.2	−0.7
F1-C7-F2	106.2(4)	106.6	106.6
C2-Si-H	113.9[d]	112.2	112.5
$(H-C-H)_{mean}$	106.1[d]	106.1	106.4
rock(C2)[c]	2.3[d]	2.3	2.4
twist(C2)[c]	1.1[d]	1.0	0.9
flap(C4) p_{10}	55.9(18)	57.1	58.2
flap(Si)	34.9(47)	38.0	38.6
ϕ(C6-Si-C2-C3) p_{11}	−37.8(54)	−42.3	−44.6
ϕ(C2-C3-C4-C5)	−64.4(18)	−65.4	−66.4
ϕ(Si-C2-C3-C4)	51.5(19)	53.8	55.4

[a] p_i: refined parameter; (p_i): the difference with parameter p_i was set to calculated value. [b] Tilt(CF_3) = $^2/_3$[(Si-C7-F1)–(Si-C7-F2)]. [c] Rock (C2) = $^1/_2$[(Si-C2-H_{eq})–(Si-C2-H_{ax}) + (C3-C2-H_{eq})–(C3-C2-H_{ax})], twist(C2) = $^1/_2$[(Si-C2-H_{eq})–(Si-C2-H_{ax})–(C3-C2-H_{eq}) + (C3-C2-H_{ax})]. [d] Not refined.

Preliminary refinements were performed with fixed vapor compositions. The plot of the *R* factors versus percentage of axial conformer **5a** is shown in Figure 3. The best agreement between experimental and calculated sM(*s*) functions was achieved at the ratio of axial and equatorial conformers of 56:44. The uncertainty in the vapor composition was estimated by Hamilton's method[22] and was found to be 16% at the significance level of 0.05 (see Figure 3). Simultaneous refinement of geometric parameters, vibrational amplitudes and vapor composition gave the ratio of 58(12):42(12) (uncertainty is $3\sigma_{LS}$ value) with $R_f = 5.4\%$. Four correlation coefficients had values larger than 0.7: $p_2/p_1 = 0.72$, $p_6/p_8 = 0.70$, $p_6/p_{11} = 0.78$, $p_4/p_9 = 0.79$.

The experimental structural parameters for the prevailing axial conformer **5a** together with the calculated values are listed in Table 1. In addition to the refined independent parameters, a few important dependent parameters are also shown in Table 1. Interatomic distances, experimental and calculated vibrational amplitudes and vibrational corrections (without nonbonded distances involving hydrogen atoms)

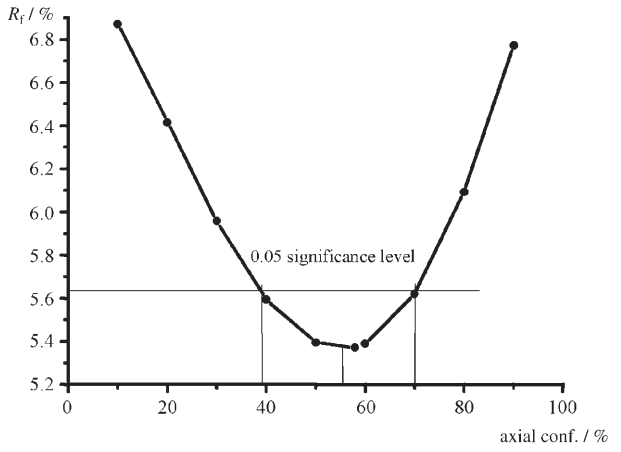

Figure 3. Agreement factor R_f for different contributions of axial conformer **5a**.

are listed in Table 2. The difference between experimental and calculated sM(s) and f(r) functions are shown in Figure 2.

The molecular structure of the axial and equatorial conformers of **5** was analyzed by two different computational methods (B3LYP and MP2 with the 6-31G** basis set). Both methods result in similar geometric parameters for the **5a** and **5e** conformers. The results for **5a** are shown in Table 1. The MP2 approximation predicts the Si–C and the C–C bond lengths about 0.009 Å shorter than the B3LYP method with the same differences between Si–C2/Si–C7 and C2–C4/C3–C4 bonds. Both quantum chemical methods reproduce the experimental structure satisfactorily, except for the Si–C2 bond length and ΔSiC. Both methods predict the Si–C2 too long and the ΔSiC too short (see Table 1). The experimental and calculated puckering parameters of a six-membered ring agree within error limit.

The important geometric ring parameters of equatorial conformers $C_5H_{10}SiHCF_3$ **5e** and $C_5H_{10}SiHCH_3$ **4e** and silacyclohexane **6** are compared in Table 3.[23] The ring Si–C bond length decreases in **6**–**4e**–**5e** series possibly due to the increase of the electronegativity, χ, of the terminal (exocyclic) substituent ($\chi_H = 2.08$,[24] $\chi_{CH_3} = 2.56$,[25] $\chi_{CF_3} = 3.46$–3.55[26]) as it takes place within the series of 1,1-disubstituted silacyclobutanes.[27] The value of flap (C4) angle does not change under terminal substituent influence in contrast to value of flap(Si).

The Si–C bond length depends strongly on the substituents at silicon and carbon atoms and varies in a wide range of 1.82–1.94 Å.[28] Notable examples are the large difference between Si–C2/Si–C7 and the extra long Si–C7 bond in **5**.

Table 2. Interatomic distances, experimental and calculated vibrational amplitudes and vibrational corrections (without nonbonded distances involving hydrogen atoms) for axial conformer **5a** [Å].[a]

	r_a	l_{exptl}	l_{calcd}[c]	$\Delta r = r_{h1} - r_a$	Group[d]
C–H	1.116	0.074(5)[b]	0.077	0.0054	1
C7–F1	1.358	0.048(2)	0.046	0.0016	2
C7–F2	1.352	0.047(2)	0.045	0.0016	2
C2–C3	1.545	0.049(2)	0.053	0.0018	3
C3–C4	1.537	0.048(2)	0.052	0.0015	3
Si–H	1.482	0.085(2)	0.089	0.0052	3
Si–C2	1.855	0.050(5)	0.053	0.0017	4
Si–C7	1.933	0.050(5)	0.053	0.0014	4
F1···F2	2.166	0.061(2)	0.059	0.0047	5
F2···F3	2.161	0.060(2)	0.058	0.0041	5
C2···C4	2.587	0.066(6)	0.071	0.0066	6
C3···C5	2.569	0.064(6)	0.069	0.0063	6
Si···F2	2.747	0.079(6)	0.084	0.0064	6
Si···F1	2.752	0.078(6)	0.083	0.0063	6
Si···C3	2.824	0.069(6)	0.074	0.0084	6
C2···C6	2.971	0.058(27)	0.084	0.0080	7
C2···C7	3.063	0.079(27)	0.105	0.0084	7
C2···C5	3.162	0.084(9)	0.082	0.0098	8
Si···C4	3.193	0.079(9)	0.077	0.0104	8
C2···F1	3.385	0.223(9)	0.221	0.0108	8
C2···F2	3.423	0.244(18)	0.250	0.0160	9
C3···F1	3.447	0.266(18)	0.272	−0.0066	9
C3···C7	3.679	0.163(18)	0.169	0.0180	9
C4···F1	4.021	0.255(15)	0.246	−0.0103	10
C3···F2	4.234	0.331(15)	0.322	0.0463	10
C2···F3	4.239	0.103(15)	0.094	0.0364	10
C4···C7	4.280	0.165(15)	0.156	0.0212	10
C3···F3	4.835	0.191(45)	0.197	0.0536	11
C4···F2	5.170	0.246(45)	0.252	0.0530	11

[a] For atom numbering see Figure 1. [b] Error limits are $3\sigma_{LS}$ values. [c] B3LYP/6-31G**. [d] Group of refined amplitudes.

This phenomenon can be explained by means of the electrostatic scheme. According to the B3LYP calculation, the Mulliken atomic charges (with hydrogens summed into heavy atoms) of **5e** are $q(C2) = -0.09$, $q(Si) = 0.46$, and $q(C7) = 0.32$. The large positive charge on the C7 atom due to its fluorination causes electrostatic repulsive interaction between the C7 and Si atoms, in contrast of attractive interaction be-

Table 3. Comparison of geometric parameters of silacyclohexane **6**, and of equatorial conformers 1-methyl-1-silacyclohexane **4e** and 1-trifluoromethyl-1-silacyclohexane **5e**.

	5e this work GED r_{h1}-structure	**5e** this work B3LYP/6-31G** r_e structure	**6** ref. [23] GED r_g structure	**4e** ref. [1] GED r_a structure
Si–C2	1.856(3)	1.885	1.885(3)	1.867(4)
Si–C7	1.934(10)	1.931	–	1.862(4)
$(C–C)_{mean}$	1.542(2)	1.544	1.550(3)	1.531(2)
$(C–H)_{mean}$	1.121(5)	1.098	1.115(5)	1.104(3)
C2-Si-C6	106.4(18)	106.3	104.2(14)	102.8(20)
Si-C2-C3	111.9(10)	110.4	110.6(6)	110.5(16)
C2-Si-C7	109.7(9)	110.5	–	112.5(24)
flap(C4)	55.8(18)	57.0	58.7(15)	55.9(20)
flap(Si)	36.5(47)	39.6	41.3(41)	46.0(31)
ϕ(C6-Si-C2-C3)	−39.5(54)	−42.3	−44.0(42)	−49.8(28)
ϕ(C2-C3-C4-C5)	−64.3(18)	−65.4	−67.5(20)	−62.9(9)
ϕ(Si-C2-C3-C4)	52.3(19)	53.8	57.3(20)	56.6(10)

tween C2 and Si. Thus, the Si–C2 bond becomes a little shorter than the Stevenson–Schomaker corrected sum of the covalent radii for silicon and carbon atoms (1.877 Å), and the Si–C7 bond is considerably longer than this sum.

According to the GED data the concentration of the axial conformer **5a** in the vapor of **5** at 293 K is 58(12) mol%. This value corresponds to an A value of −0.19(29) kcal mol^{-1} (Table 4).

Table 4. Conformational properties of $C_5H_{10}SiHCF_3$ (**5**).

Method	T/K	$\Delta E = E_{ax} - E_{eq}$ [kcal mol^{-1}]	$A = G_{ax} - G_{eq}$ [kcal mol^{-1}]	mol% axial
B3LYP/6-31G**	298	−0.30	−0.01	50
MP2/6-31G**	298	−0.58	−0.23	59
CBS-QB3	298	−0.61	−0.27	61
CBS-QB3	115	−0.57	−0.48	89
IPCM(B3LYP/6-311G*)[a]	298	+0.45	+0.58	27
IPCM(B3LYP/6-311G*)[a]	115	+0.49	+0.40	15
IPCM(B3LYP/6-311G*)[b]	298	+0.17	+0.44	32
IPCM(B3LYP/6-311G*)[b]	115	+0.21	+0.27	23
GED	293		−0.19(29)	58(12)
NMR[c]	113		+0.4(1)	17(2)

[a] CBS-QB3 results with solvent effects calculated for a CH_2Cl_2 solution. [b] CBS-QB3 results with solvent effects calculated for a $CHCl_3$ solution. [c] Measured in a 1:1:3 mixture of CD_2Cl_2, $CHFCl_2$, and CHF_2Cl.

NMR Spectroscopy: The ^{19}F NMR spectra at room temperature and down to 138 K show rapid interconversion of **5e** and **5a**. On cooling to 128 K, the spectrum (Figure 4) shows

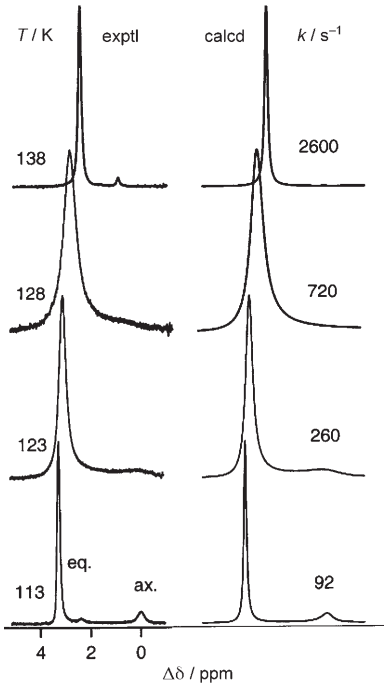

Figure 4. Simulation of ^{19}F NMR spectra for **5**. Experimental spectra left and calculated right. Solvent is a 1:1:3 mixture of CD_2Cl_2, $CHFCl_2$, and CHF_2Cl. A small peak to the right of the main signal, visible in spectra at 138 and 113 K, is due to impurities in the sample.

line broadening and at 123 K signal splitting has occurred resulting in a main signal and a smaller one at higher field, indicating a mixture of a major and a minor conformer. As a general rule in cyclohexane chemistry, the resonance signal of a substituent in axial position has a lower δ value than the signal for the same substituent in equatorial position.[29,30] Therefore, the main signal is assigned to the equatorial conformer **5e**. This assignment is further supported by GIAO calculations[31] for **5e** and **5a**. At the B3LYP/6-311+G** level of theory, **5a** is predicted to have a 3.6 ppm lower ^{19}F chemical shift than **5e**, which is in excellent agreement with the experimental signal separation at 113 K (see Figure 4). DNMR simulations of the spectra allowed the determination of the rate constants and equilibrium constants (hence free energy changes) for the equatorial to axial transformations as well as the corresponding free energies of activation as a function of temperature. The rate constants used to simulate the experimental spectra yielded $\Delta G^{\neq} = 5.5(2)$ kcal mol^{-1}. At 113 K, values of $K = 0.2$ and $\Delta G = 0.4(1)$ kcal mol^{-1} were obtained (Table 4). A precise temperature dependence of K and ΔG for the narrow temperature range 108–138 K could not be determined.

Computational details: All calculations were carried out using the Gaussian98 and Gaussian03 program packages.[32,33] Parallel to the GED analysis, geometry optimizations of the equatorial and axial conformer of **5** were performed with the hybrid DFT functional B3LYP, and the MP2 approximation, both with the 6-31G** basis sets, and with the CBS-QB3 method as implemented in Gaussian03.[34,35] All three methods predict lower energies for the axial form between −0.30 and −0.61 kcal mol^{-1} and free energies near zero or slightly negative (Table 4). The geometric parameters of the axial form are listed in Table 1 together with the experimental results. When the results of the two experimental methods (GED and ^{19}F NMR) were compared, there appeared to be a discrepancy in their findings regarding the conformational equilibrium of **5**. Therefore additional calculations were carried out, which take into account the solvent effect in solution and the temperature dependence both in solution and in the gas phase. The minimum energy path for the chair-to-chair inversion of **4** and **5** in internal redundant coordinates was also calculated using the Synchronous Transit-Guided Quasi-Newton (STQN) method[36] at the B3LYP/6-311+G** level of theory. The effect of solvation in dichloromethane and in chloroform on the free energy difference for the chair-to-chair inversion was calculated at the B3LYP/6-311G* and IPCM(B3LYP/6-311G*) (Static Isodensity Surface Polarized Surface Continuum Model)[37] levels of theory, with solvational geometry relaxation and zero point energies taken into account with the PCM(B3LYP/6-311G*) (Polarizabale Continuum Model)[38] method.

Computational studies in the gas phase: The minimum energy pathway for the chair-to-chair inversion of the unsubstituted silacyclohexane ring **6** has been shown to consist

of a half-chair/sofa like transition state from which the molecule can move into a twist form of relatively high energy. Then the molecule goes through a boat form into a more stable twist form, which marks the midpoint on the symmetrical path. In order to complete the inversion, the molecule has to go further through a boat, twist, and half-chair/sofa transition state before it ends up in the inverted chair.[39,40]

The minima and the transition states along the minimum energy path for **5**, from the axial to the equatorial conformer, were located using the STQN(Path) method as implemented in Gaussian03[36] at the B3LYP/6-311+G** level of theory. The reaction path was calculated in four slices using the keyword OPT(QST3,PATH=11), that is, from minimum **5a** to **5b**, from **5b** to **5c**, from **5c** to **5d**, and from **5d** to **5e**, as shown in Figure 5. For comparison, the conformational

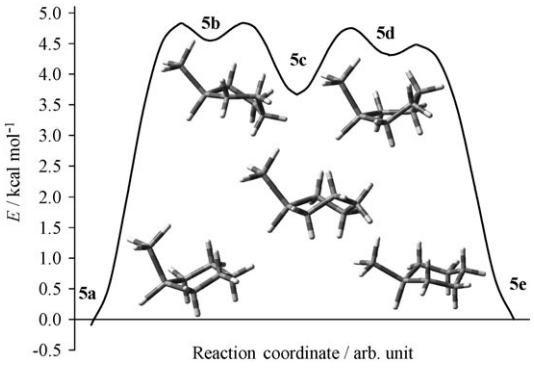

Figure 5. Calculated minimum energy path in internal redundant coordinates for the chair-chair inversion of **5** at the B3LYP/6-311+G** level of theory.

path was also calculated for the methyl-substituted silacyclohexane **4**. The results are summarized in Table 5. For both compounds, **5** and **4**, the inversion path resembles the one for **6**; the deviation from the symmetrical path for **6** is in each case caused by the substituent.

The electronic energy of activation in the gas-phase between minima **5b** and **5c**, is calculated to be 4.92 kcal mol^{-1} (relative to **5a**), which is marginally lower than the free energy of activation derived from NMR data in solution.

The gas-phase $\Delta G^{298\,K}$ of ring inversion was found to be -0.27 kcal mol^{-1} with the CBS-QB3 method of Petersson et al.[34,35] Based on this value, the constant of equilibrium is $K=0.63$ at room temperature, and the ratio of the axial conformer is 61 % of the total, in good agreement with the electron diffraction experiment (Table 4).

The effect of CF_3 internal rotation was also evaluated based on the harmonic vibrational frequency corresponding to internal rotation (B3LYP/6-311G* frequencies are 37.5 cm^{-1} in the axial and 32.8 cm^{-1} in the equatorial conformer), and the barrier to internal rotation (1.38 kcal mol^{-1} in the axial and 1.52 kcal mol^{-1} in the equatorial conformer, obtained by scanning one C-Si-C-F dihedral angle and carrying out constrained optimizations) and a density-of-states interpolation function by McClurg, Flagan and Goddard III[41] as corrected by Knyazev.[42] The correction to the free energy of inversion was found to be negligible as it increases from 0.004 kcal mol^{-1} at 100 K to -0.008 kcal mol^{-1} at 298 K.

Computational studies in solution: Solvation effects were calculated with the PCM(B3LYP/6-311G*) and IPCM-(B3LYP/6-311G*) models together with gas phase B3LYP/6-311G* calculations, and were added as corrections to the room temperature CBS-QB3 results for the conformational inversion. The PCM method[38] was used to study the geometry relaxation and the changes in the zero-point energy correction. Single point IPCM[37] energies were calculated at the relaxed geometries. We used dichloromethane and chloroform as solvents, as these are parameterized in the PCM model, and are believed to resemble the actual solvent mixture. From the dielectric constants of the solvents involved (CH_2Cl_2 (9.1); CHF_2Cl (6.1); $CHFCl_2$ (unknown); $CHCl_3$ (4.8)) there is a reason to believe that CH_2Cl_2 represents an upper limit and that $CHCl_3$ represents a lower limit of the solvation effects in the freon mixture.

The contribution of the geometry relaxation and the change in zero-point energy to the free energy of inversion in solution is only on the order of 0.01 kcal mol^{-1}. However, the IPCM electron energy contribution to the ΔG^0 of chair-to-chair inversion is 0.8 kcal mol^{-1} in chloroform and 0.9 kcal mol^{-1} in dichloromethane at the PCM-relaxed geometries. Incorporating solvent effects in the free energy of chair-to-chair inversion, $\Delta\Delta G^0$ is expected to be around 0.85 kcal mol^{-1} between the gas and the solvent phase.

The effect of cooling on the conformational equilibrium was calculated at several temperatures using unscaled B3LYP/6-311G* and PCM(B3LYP/6-311G*) frequencies and rotational constants in the gas and in the solvent phases. The resulting curves for the temperature dependence in the interval between 100 K and 300 K are shown in Figure 6. Low (115 K) and high (298 K) temperature data are included in Table 4 for reference. For both solvents the calculations predict an increasing stability of the equatorial conformer at very low temperatures. The observation from the NMR studies, that the equatorial isomer is more stable in solution at low temperatures is thus reproduced surprisingly well by solution ab initio inversion free energies. Indeed, the equatorial ratio of **5** obtained from the

Table 5. Stationary points [kcal mol^{-1}] along the conformational inversion path for **4** and **5**.[a]

	a	(**a**–**b**)$^{\#}$[b]	**b**	(**b**–**c**)$^{\#}$	**c**	(**c**–**d**)$^{\#}$	**d**	(**d**–**e**)$^{\#}$	**e**
4	0.47	5.51	4.84	5.16	3.95	5.35	5.09	5.65	0.00
CBS-QB3	*0.35*				*3.61*				*0.00*
5	−0.09	4.82	4.54	4.83	3.66	4.75	4.31	4.47	0.00
CBS-QB3	*−0.54*				*3.20*				*0.00*

[a] The stationary points were located with the STQN method at the B3LYP/6-311+G** level of theory. Together with the B3LYP electronic energies, CBS-QB3 0 K ZPE-corrected energies are also listed for the axial, the equatorial, and the most stable twist conformer in the middle of the inversion path. [b] (**a**–**b**)$^{\#}$ is the saddle point on the inversion path between conformers **a** and **b** (Figure 5).

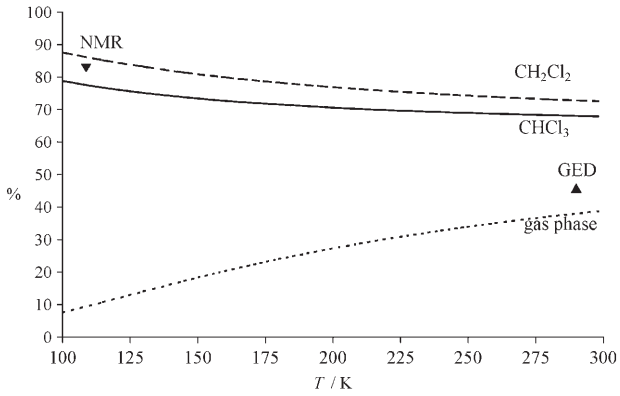

Figure 6. Calculated equatorial ratio of $C_5H_{10}SiHCF_3$, **5** in the temperature range from 100 to 300 K. The equatorial ratio is calculated for the gas phase, in a $CHCl_3$ solution, and in a CH_2Cl_2 solution. For calculation details, see text. Experimental GED and NMR results are marked on the graph.

^{19}F NMR spectra in the freon mixture lies between the calculated values for **5** in $CHCl_3$ and CH_2Cl_2.

Conclusion

The conformational equilibrium of the title compound **5** was examined by two experimental methods; by electron diffraction in the gas-phase at 293 K and by ^{19}F NMR spectroscopy in solution at temperatures down to 108 K. The GED experiment shows a slight preference for the axial conformer, whereas the equatorial conformer is preferred in the solution at low temperatures. The experimental results are remarkably well reproduced by ab initio calculations on the conformational properties of **5** in the gas-phase and in solution for the temperature range from 100 to 300 K.

The molecular structure of **5** is influenced by the CF_3 group, which makes the exocyclic Si–C bond extremely long and results in a moderate shortening of the endocyclic Si–C bonds.

Conformational properties of monosubstituted silacyclohexanes with methyl and trifluoromethyl as substituents are in striking contrast to those of the corresponding cyclohexane derivatives. For methylcyclohexane, A values of 1.8–2.0 kcal mol^{-1} have been reported,[10] whereas the A value for trifluorocyclohexane is 2.5 kcal mol^{-1}.[18] In methylsilacyclohexane, the activation energy for the ring inversion is only half of that for methylcyclohexane.[40] Therefore it is not surprising that its A value is found to be much lower than in the case of methylcyclohexane (0.4–0.6 kcal mol^{-1} in the gas-phase at room temperature; 0.2 kcal mol^{-1} in solution at 110 K).[1] The slightly negative A value found for trifluoromethylsilacyclohexane in the gas-phase is unexpected as it shows an opposite behavior of trifluoromethyl versus methyl substituents when compared with monosubstituted cyclohexanes. More work needs to be done before a thorough explanation can be given. For this purpose, we have already started to examine the conformational properties of additional monosubstituted silacyclohexanes. Obtaining a broader collection of data would be valuable in order to model this phenomenon with the help of various effects, such as hyperconjugation, which may be influence the conformational equilibrium as has recently been reported for monosubstituted cyclohexanes and heterocyclohexanes.[3,6,7]

The fact, that **5e** is more stable than **5a** in polar solvents such as methylenchloride, chloroform, and the freons used in the low-temperature ^{19}F NMR experiment, could be explained qualitatively as being due to stronger interaction, and hence stabilization, of the more polar conformer **5e** with the polar solvent molecules.

Experimental Section

Materials: Compound **5** was prepared in a slight variation to the standard preparation of F_3CSiCl_3.[43] Bromotrifluoromethane was purchased from Pfaltz & Bauer and was used without further purification. CH_2Cl_2 was dried over CaH_2. The standard Schlenk technique was used for all manipulations.

1-Trifluoromethyl-1-silacyclohexane (5): CF_3Br (5.3 g, 35.6 mmol) was condensed into a reaction flask containing cyclo-$(CH_2)_5SiHCl$ (4.52 g, 33.6 mmol) and CH_2Cl_2 (10 mL). The content of the flask was allowed to melt and its temperature was then maintained at −84 °C (ethyl acetate slush) and then a solution of $P(NEt_2)_3$ (8.31 g, 33.6 mmol) in CH_2Cl_2 (10 mL) was added slowly under stirring. Soon, the solution turned pink and then red. The cooling bath was removed and stirring was continued at room temperature overnight. All volatile components were then condensed into a trap held at −196 °C. The solvent was distilled off and the product collected at 125–126 °C and 1 atm. Further purification was achieved by trap to trap condensation on the vacuum line. The product was kept at −45 °C (chlorobenzene slush) and the volatile components were discarded. Yield: 2.27 g, 40 % (colorless liquid); ^1H NMR (250 MHz, $CDCl_3$, 25 °C, TMS): $\delta = 0.82$–1.09 (m, 4H, CH_2), 1.29–1.46 (m, 1H, $CH_{2(ax/eq)}$), 1.48–1.63 (m, 1H, $CH_{2(ax/eq)}$), 1.66–1.90 (m, 4H, CH_2), 4.06–4.18 m, 1H, SiH); ^{13}C NMR (62.9 MHz, $CDCl_3$, 25 °C, TMS): $\delta = 6.2$, 23.4, 28.7 (CH_2), 131.2 (q, CF_3, $J_{CF} = 321$ Hz); ^{19}F NMR (235 MHz, $CDCl_3$, 25 °C, $CFCl_3$): $\delta = -61.1$ (d, $^3J_{F,H} = 5.9$ Hz); ^{29}Si NMR (49.7 MHz, $CDCl_3$, 25 °C, TMS): $\delta = 18.7$; MS (EI, 70 eV): m/z (%): 99 (84) [$M^+ - CF_3$], 97 (100) [$M^+ - CF_3 - H_2$], 71 (81) [$M^+ - CF_3 - Si$].

GED Experiment: Electron diffraction intensities were recorded with a Gasdiffraktograph KD-G2[44] at 25 and 50 cm nozzle-to-plate distances and with an accelerating voltage of about 60 kV. The sample was cooled to 15 °C and the inlet system and nozzle were at room temperature. The photographic plates were analyzed with an Agfa Duoscan HiD scanner and total scattering intensity curves were obtained from the TIFF-file using the program SCAN3.[45] Experimental molecular intensities were obtained in the range $s = 2$–18.2 and 8–35.4 Å^{-1} with steps $\Delta s = 0.2$ Å^{-1} for the long and short camera distances, respectively, ($s = (4\pi/\lambda)\sin\theta/2$, where λ is the electron wavelength and θ is the scattering angle). sM(s) as shown in Figure 7 was obtained by splicing the functions for the long and the short nozzle-to-plate distances. A weight function $w = \exp(-0.05 \cdot (30.4 - s_i)^2)$ was applied to decrease the noise contribution in the region $s = 30.4$–35.4 Å^{-1}.

Low-temperature NMR experiment: A solvent mixture of CD_2Cl_2, $CHFCl_2$, and CHF_2Cl in a ratio of 1:1:3 was used for the ^{19}F NMR measurements at very low temperatures. The temperatures of the probe were calibrated by means of a type K (Chromel/Alumel) thermocouple inserted into a dummy tube the day before and the day after the NMR experiment. The low-temperature measurements are estimated to be accurate to ±2 K. Spectra were loaded into the data-handling program IGOR (WaveMetrics) for analysis, manipulations, and graphic display. Line shape simulations of the NMR spectra were performed by use of a PC version of the DNMR program (QCPE program no. 633; Indiana University, Bloomington, IN), kindly offered by professor L. Lunazzi.[46]

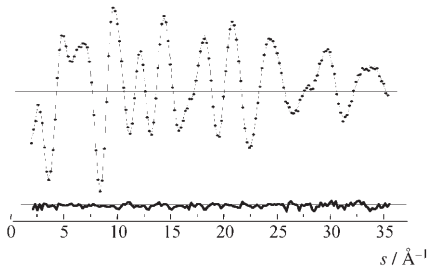

Figure 7. Experimental (•••••) and calculated (——) molecular intensities and residual for mixture of **5a** and **5e**.

Acknowledgements

We thank the Deutsche Forschungsgemeinschaft and the Russian Foundation for Basic Researches for financial support of the Russian-German Cooperation (413 RUS 113/69, 05-03-04003 DFG a) including a fellowship for N.I.G. and G.V.G. A fellowship from DAAD is gratefully acknowledged by G.V.G. We would also like to acknowledge the computational facilities made available by Prof. Paul Mezey, Director, Scientific Modeling and Simulation Laboratory (SMSL), Memorial University of Newfoundland.

[1] I. Arnason, A. Kvaran, S. Jonsdottir, P. I. Gudnason, H. Oberhammer, *J. Org. Chem.* **2002**, *67*, 3827–3831.
[2] I. V. Alabugin, *J. Org. Chem.* **2000**, *65*, 3910–3919.
[3] I. V. Alabugin, T. A. Zeidan, *J. Am. Chem. Soc.* **2002**, *124*, 3175–3185.
[4] G. Cuevas, E. Juaristi, *J. Am. Chem. Soc.* **2002**, *124*, 13088–13096.
[5] N. Leventis, S. B. Hanna, C. Sotiriou-Leventis, *J. Chem. Educ.* **1997**, *74*, 813–814.
[6] D. S. Ribeiro, R. Rittner, *J. Org. Chem.* **2003**, *68*, 6780–6787.
[7] F. Taddei, E. Kleinpeter, *J. Mol. Struct. (Theochem)* **2004**, *683*, 29–41.
[8] F. Taddei, E. Kleinpeter, *J. Mol. Struct. (Theochem)* **2005**, *718*, 141–151.
[9] C. H. Bushweller in *Conformational Behavior of Six-Membered Rings* (Ed. E. Juaristi), VCH, New York, **1995**, pp. 25–58.
[10] K. B. Wiberg, J. D. Hammer, H. Castejon, W. F. Bailey, E. L. DeLeon, R. M. Jarret, *J. Org. Chem.* **1999**, *64*, 2085–2095.
[11] K. G. Penman, W. Kitching, W. Adcock, *J. Org. Chem.* **1989**, *54*, 5390–5391.
[12] Q. Shen, S. Rhodes, J. C. Cochran, *Organometallics* **1992**, *11*, 485–486.
[13] S. G. Cho, O. K. Rim, Y.-S. Kim, *J. Mol. Struct. (Theochem)* **1996**, *364*, 59–68.
[14] R. Carleer, M. J. O. Anteunis, *Org. Magn. Reson.* **1979**, *12*, 673–678.
[15] M. R. Frierson, M. R. Iman, V. B. Zalkow, N. L. Allinger, *J. Org. Chem.* **1988**, *53*, 5248–5258.
[16] R. J. Ouellette, *J. Am. Chem. Soc.* **1974**, *96*, 2421–2425.
[17] I. Arnason, H. Oberhammer, *J. Phys. Chem. A* **2003**, *107*, 243–247.
[18] E. W. Della, *J. Am. Chem. Soc.* **1967**, *89*, 5221–5224.
[19] B. Andersen, H. M. Seip, T. G. Strand, R. Stolevik, *Acta Chem. Scand.* **1969**, *23*, 3224–3224.
[20] A. W. Ross, M. Fink, R. L. Hilderbrandt, *International Tables of Crystallography, Vol. C*, Kluwer Acad. Publ., Dordrecht, **1992**, p. 245.
[21] V. A. Sipachev, *J. Mol. Struct.* **2001**, *567–568*, 67–72.
[22] W. C. Hamilton, *Acta Crystallogr.* **1965**, *18*, 502–510.
[23] Q. Shen, R. L. Hilderbrandt, V. S. Mastryukov, *J. Mol. Struct.* **1979**, *54*, 121–134.
[24] R. J. Boyd, K. E. Edgecombe, *J. Am. Chem. Soc.* **1988**, *110*, 4182–4186.
[25] C. A. Brookman, S. Cradock, D. W. H. Rankin, N. Robertson, P. Vefghi, *J. Mol. Struct.* **1990**, *216*, 191–200.
[26] A. Haas, *J. Fluorine Chem.* **1999**, *100*, 21–34.
[27] M. Dakkouri, M. Grosser, *J. Mol. Struct.* **2002**, *610*, 159–174.
[28] Landoldt-Börnstein, *Structure Data of Free Polyatomic Molecules, Group II, Vols. 7, 15, 21 and 23*, Springer, Berlin.
[29] H. Booth in *Progress in NMR Spectroscopy, Vol. V* (Eds.: J. W. Emsley, J. Feeney, L. H. Sutcliffe), Pergamon Press, Oxford, **1969**, p. 240.
[30] H.-O. Kalinowski, S. Berger, S. Braun in *^{13}C NMR-Spektroskopie*, Thieme, Stuttgart/New York, **1984**.
[31] K. Wolinski, J. F. Hinton, P. Pulay, *J. Am. Chem. Soc.* **1990**, *112*, 8251–8260.
[32] Gaussian 03, Revision C.02, M. J. Frisch, G. W. Trucks, H. B. Schlegel, G. E. Scuseria, M. A. Robb, J. R. Cheeseman, J. J. A. Montgomery, T. Vreven, K. N. Kudin, J. C. Burant, J. M. Millam, S. S. Iyengar, J. Tomasi, V. Barone, B. Mennucci, M. Cossi, G. Scalmani, N. Rega, G. A. Petersson, H. Nakatsuji, M. Hada, M. Ehara, K. Toyota, R. Fukuda, J. Hasegawa, M. Ishida, T. Nakajima, Y. Honda, O. Kitao, H. Nakai, M. Klene, X. Li, J. E. Knox, H. P. Hratchian, J. B. Cross, V. Bakken, C. Adamo, J. Jaramillo, R. Gomperts, R. E. Stratmann, O. Yazyev, A. J. Austin, R. Cammi, C. Pomelli, J. W. Ochterski, P. Y. Ayala, K. Morokuma, G. A. Voth, P. Salvador, J. J. Dannenberg, V. G. Zakrzewski, S. Dapprich, A. D. Daniels, M. C. Strain, O. Farkas, D. K. Malick, A. D. Rabuck, K. Raghavachari, J. B. Foresman, J. V. Ortiz, Q. Cui, A. G. Baboul, S. Clifford, J. Cioslowski, B. B. Stefanov, G. Liu, A. Liashenko, P. Piskorz, I. Komaromi, R. L. Martin, D. J. Fox, T. Keith, M. A. Al-Laham, C. Y. Peng, A. Nanayakkara, M. Challacombe, P. M. W. Gill, B. Johnson, W. Chen, M. W. Wong, C. Gonzalez and J. A. Pople, Gaussian, Inc., Wallingford CT, **2004**.
[33] Gaussian 98, Revision A.6, M. J. Frisch, G. W. Trucks, H. B. Schlegel, G. E. Scuseria, M. A. Robb, J. R. Cheeseman, V. G. Zakrzewski, J. A. Montgomery, R. E. Stratmann, J. C. Burant, S. Dapprich, J. M. Millam, A. D. Daniels, K. N. Kudin, M. C. Strain, O. Farkas, J. Tomasi, V. Barone, M. Cossi, R. Cammi, B. Mennucci, C. Pomelli, C. Adamo, S. Clifford, J. Ochterski, G. A. Petersson, P. Y. Ayala, Q. Cui, K. Morokuma, D. K. Malick, A. D. Rabuck, K. Raghavachari, J. B. Foresman, J. Cioslowski, J. V. Ortiz, B. B. Stefanov, G. Liu, A. Liashenko, P. Piskorz, I. Komaromi, R. Gomperts, R. L. Martin, D. J. Fox, T. Keith, M. A. Al-Laham, C. Y. Peng, A. Nanayakkara, C. Gonzalez, M. Challacombe, P. M. W. Gill, B. Johnson, W. Chen, M. W. Wong, J. L. Andres, M. Head-Gordon, E. S. Replogle and J. A. Pople, Gaussian, Inc., Pittsburgh PA, **1998**.
[34] J. A. Montgomery Jr., M. J. Frisch, J. W. Ochterski, G. A. Peterson, *J. Chem. Phys.* **1999**, *110*, 2822–2827.
[35] J. A. Montgomery Jr., M. J. Frisch, J. W. Ochterski, G. A. Peterson, *J. Chem. Phys.* **2000**, *112*, 6532–6542.
[36] P. Y. Ayala, H. B. Schlegel, *J. Chem. Phys.* **1997**, *107*, 375–384.
[37] J. B. Foresman, T. A. Keith, K. B. Wiberg, J. Snoonian, M. J. Frisch, *J. Phys. Chem.* **1996**, *100*, 16098–16104.
[38] V. Barone, M. Cossi, J. Tomasi, *J. Comput. Chem.* **1998**, *19*, 404–417.
[39] I. Arnason, Á. Kvaran, A. Bodi, *Int. J. Quantum Chem.* **2006**, *106*, 1975–1978.
[40] I. Arnason, G. K. Thorarinsson, E. Matern, *Z. Anorg. Allg. Chem.* **2000**, *626*, 853–862.
[41] R. B. McClurg, R. C. Flagan, W. A. I. Goddard, *J. Chem. Phys.* **1997**, *106*, 6675–6680.
[42] V. D. Knyazev, *J. Chem. Phys.* **1999**, *111*, 7161–7162.
[43] H. Beckers, H. Bürger, P. Bursch, I. Ruppert, *J. Organomet. Chem.* **1986**, *316*, 41–50.
[44] H. Oberhammer, *Molecular Structure by Diffraction Methods*, The Chemical Society, London, **1976**, p. 24.
[45] E. G. Atavin, L. V. Vilkov, *Instrum. Exp. Tech.* **2002**, *45*, 745–757.
[46] Courtesy of Professor sL. Lunazzi, University of Bologna (Italy).

Received: May 16, 2006
Published online: November 23, 2006

